International Journal of Advanced Geosciences, 14 (1) (2026) 1-9

International Journal of Advanced Geosciences

Website: www.sciencepubco.com/index.php/IJAG
https://doi.org/10.14419/ypbgqh87
Research paper

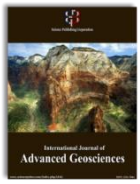

Effect of Shale on CO_2 Sequestration: A Petrophysical And Geochemical Assessment in G-Oil Field of The Niger Delta Basin

Isaac Owoicho Agada [1] *, Magnus Uzoma Igboekwe [1], Chukwunenyoke Amos-Uhegbu [2], Paul Igienekpeme Aigba [1]

[1] Department of Physics, Michael Okpara University of Agriculture, Umudike, P.M.B 7267, Umuahia, Abia State, Nigeria
[2] Department of Geology, Michael Okpara University of Agriculture, Umudike, P.M.B 7267, Umuahia, Abia State, Nigeria
**Corresponding author E-mail: agadaisaac45@gmail.com*

Received: December 1, 2025, Accepted: January 13, 2026, Published: January 18, 2026

Abstract

This research was designed to analyse the effect of Shale in CO_2 storage process petrophysically and geochemically within the G-Oil field in the Niger Delta Basin. Eight wells were profiled with 18 reservoirs delineated using Interactive Petrophysics software. Results show that Total porosity ($\emptyset_t$) within the range of 0.144-0.288 is higher than Effective Porosity ($\emptyset_{eff}$) which ranged from 0.142-0.275. Archie Water Saturation values (0.14-0.467) are higher than those of the Indonesian model (0.131-0.457). Permeability (k) values ranged from 181.01mD to 7942.091mD. Shale Volume (V_{sh}) ranged from 0.005-0.322 representing 'clean/shaly sand', with 13 reservoirs having 'shaly sand' lithology. Shale is petrophysically confirmed with a mean value of $\emptyset_t$ (0.24) higher than $\emptyset_{eff}$ (0.228), and Archie S_w (0.352) being higher than Indonesian S_w (0.31). A high mean value of k (1780.941mD) confirms the existence of highly connected pores for CO2 movement. Mean V_{sh} is 11.7%, indicating shaly sand lithology. Geochemical interaction of this shale with Dihydrogen Carbonate produced from the CO_2/H_2O reaction will increase $\emptyset$eff and k in the presence of adequate S_w (0.31). An increase in values of $\emptyset_{eff}$ and k implies an increase in storage capacity of the reservoirs such that connected micropores increase while unconnected nanopores decrease.

Keywords: *Reservoir; Shale; Permeability; Water Saturation; Porosity.*

1. Introduction

Geologic carbon sequestration involves the capture of CO_2 from atmospheric and point sources. This is followed by conversion to a supercritical phase, transportation to designated sites, and injection into subsurface reservoirs for enhanced oil recovery (EOR) and long-term storage [1–3]. The performance of this process is governed by several geological and petrophysical factors, including reservoir lithology, heterogeneity, and the presence of shale. Shale plays an important role in both hydrocarbon production and CO_2 storage systems [4]. Beyond its fine role as a caprock, shale occurring within the reservoir matrix introduces complexities that directly influence carbon storage efficiency. Its impact on reservoir properties such as porosity, permeability, and water saturation is particularly significant due to the pronounced variability in shale petrophysical characteristics [4]. Accurate characterisation of these properties is therefore essential for applied prediction of CO_2 behaviour in shale-bearing reservoirs [4], [5].

In the context of this study, reservoir shale refers to shale layers interbedded within the reservoir matrix. Where the dominant reservoir lithology is sandstone, such formations are classified as shaly sandstone reservoirs [6].

Recent studies have focused on the interaction between CO_2 and reservoir shale and the resulting changes in production-relevant parameters, particularly porosity and permeability. However, reported findings remain inconsistent, reflecting variations in experimental conditions, mineralogical composition, and fluid systems [7], [8]. To improve understanding of these interactions, [9] conducted a detailed investigation using shale core samples from selected oil reservoirs, examining coupled CO_2–brine–shale processes. Their results are broadly consistent with earlier studies [7], [8], despite differences in experimental design. Under supercritical conditions and varying moisture contents, CO_2 injection for EOR or storage was observed to alter pore structure and connectivity.

From an applied geochemical perspective, CO_2–shale interactions can induce changes in reservoir porosity and permeability through reactions between CO_2 and carbonate minerals within the shale. These reactions have direct implications for reservoir performance, injectivity, and long-term storage integrity, underscoring the importance of integrating geochemical effects into reservoir evaluation and carbon sequestration assessments.

As presented by [9] the geochemistry witnesses both forward and reverse reactions as seen in the equations below:

$$CO_{2(supercritical)} <\!\!\longrightarrow CO_{2(aq)} \quad (1)$$

$$CO_{2(aq)} + H_2O <\!\!\longrightarrow H_2CO_{3(aq)} \quad (2)$$

$$H_2CO_{3(aq)} <\!\!\longrightarrow HCO_3^-{}_{(aq)} + H^+_{(aq)} \quad (3)$$

$$CaCO_{3(s)} + H^+_{(aq)} <\!\!\longrightarrow HCO_3^-(aq) + Ca^{2+}_{(aq)} \quad (4)$$

$$HCO_3^-{}_{(aq)} + Ca^{2+}_{(aq)} <\!\!\longrightarrow CaCO_{3(s)} + H^+_{(aq)} \quad (5)$$

The reactions described in Equations (1)–(5) illustrate the geochemical mechanisms through which key reservoir production parameters are modified during CO_2 injection. These reactions are reversible and are initiated when injected or connate CO_2 dissolves in formation water to form Dihydrogen Carbonate acid (H_2CO_2). Under reservoir temperature conditions, H_2CO_2 partially dissociates, producing hydrogen ions (H^+) in aqueous solution. These hydrogen ions subsequently react with carbonate minerals, particularly calcium carbonate present in shale. This reaction releases calcium ions (Ca^{2+}), which may recombine with bicarbonate ions (HCO_3^-) to precipitate calcium carbonate and regenerate hydrogen ions. The forward and reverse reactions continue over extended periods until chemical equilibrium is reached. At equilibrium, the reservoir system stabilises, contributing to the long-term retention of stored CO_2 through solubility and mineral trapping mechanisms [7–9].

These reactions are particularly relevant to this study because they directly influence solubility trapping and are strongly controlled by shale volume, water saturation, porosity, and permeability. Shale volume is a key focus of this research due to its direct impact on petrophysical and production-related reservoir parameters. Previous studies [10], [11] have identified distinct shale volume classifications and demonstrated their influence on reservoir performance.

This study was designed to evaluate the influence of shale on the carbon sequestration process within the G-Oil Field, Niger Delta Basin. The findings are intended to provide applied insights that may support informed decision-making and investment in carbon sequestration initiatives within the region.

1.1. Study location

The study area, G-Oil Field, is located within the Greater Ughelli depobelt of the Niger Delta Basin, between latitudes 4°N and 6°N and longitudes 5°E and 8°E [12], [13]. The field covers an area of approximately 36.9 km². The spatial distribution of the eight wells analysed in this study is shown in Fig. 1.

The Niger Delta Basin is underlain by three major lithostratigraphic units: the Benin, Agbada, and Akata Formations [14]. These formations, ranging in age from early Tertiary to Recent [15, 16], control the basin's reservoir characteristics and hydrocarbon distribution. The basin comprises five depobelts—Northern Delta, Greater Ughelli, Central Swamp, Coastal Swamp, and Offshore—which represent successive depositional sequences. The interbedded shale–sandstone architecture of the Agbada Formation, together with the thick Akata shale, accounts for the basin's high hydrocarbon prospectivity and its suitability for carbon sequestration applications [16].

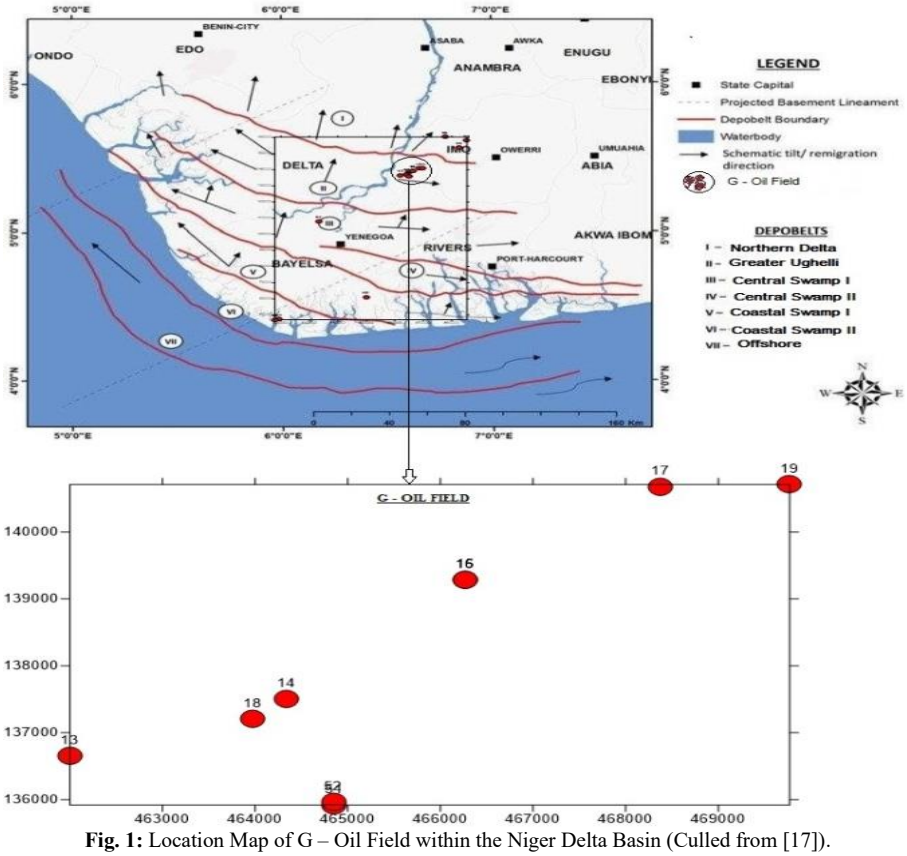

Fig. 1: Location Map of G – Oil Field within the Niger Delta Basin (Culled from [17]).

2. Material and Methods

Materials used in this study include wireline well log data in American Standard Code for Information Interchange (ASCII) format and Interactive Petrophysics (IP) software for petrophysical analysis. Surfer® 13 software was used for spatial mapping, while Microsoft Excel was employed for statistical analysis. A total of eight (8) wells within the G-Oil Field were analysed.
Petrophysical properties of interest—porosity, permeability, water saturation, and shale volume—were evaluated using a standardised IP workflow that allows for systematic documentation of applied algorithms and processing steps. Well log data were imported into the IP environment, where the workspace was configured, normalised, and displayed using appropriate log tracks. Log curves were selected based on the specific analytical objectives.
Reservoir identification and correlation were performed using relevant individual and combined logs. Reservoir intervals were delineated using cutoff and summation algorithms implemented within the IP software, ensuring consistent and accurate reservoir definition. This process resulted in the identification of potential reservoir units and hydrocarbon-bearing zones, represented as reservoir and pay flags in the reservoir models (Appendices 1–8).
Petrophysical properties such as Total and Effective porosities were analyzed using Tixier equations (6) and (7) respectively [18].

$$\text{Porosity } (\emptyset) = \frac{\rho_{ma} - \rho_b}{\rho_{ma} - \rho_{fl}} \tag{6}$$

$$\text{Effective Porosity } (\emptyset_{eff}) = \emptyset_t\ (1 - V_{sh}) \tag{7}$$

Where ρ_{ma} is matrix density, ρ_b bulk density, ρ_{fl} is fluid density, $\emptyset_t$ is total porosity and V_{sh} is Shale volume.
[17] classified porosity qualitatively into 5 categories: $\emptyset \leq 5\%$ is considered negligible while $5\% < \emptyset \leq 10\%$ is weak porosity. Porosity in the range $10\% < \emptyset \leq 15\%$ is medium porosity while $15\% < \emptyset \leq 20\%$ is considered as good porosity. Porosity in the range $20\% < \emptyset \leq 40\%$) constitutes a very good porosity.
Permeability was obtained using Wiley-Rose model in equations (8) considering the application of porosity as fraction [18].

$$k = a\left[\frac{\emptyset^b}{S_{wirr}{}^c}\right] \tag{8}$$

Where k is permeability; a, b and c are constants, while S_{wirr} is irreducible water saturation.
According to [17], qualitative classification of permeability reads: ≤ 10 mD is poor permeability, $10 < k \leq 100$ mD is fair, $100 < k \leq 1000$ mD is good while $k > 1000$ mD is Excellent. Note that mD is millidarcy (Unit of permeability).
Indonesian model in equation (9) [19] was used to determine Water saturation (S_w).

$$\frac{1}{\sqrt{R_t}} = \left[\frac{V_{sh}^{1-\frac{V_{sh}}{2}}}{\sqrt{R_{sh}}} + \frac{\emptyset_{eff}}{\sqrt{R_t}}\right] * S_w \tag{9}$$

Where R_t is true resistivity of formation, R_{sh} is resistivity of shale,
Values of $S_w \leq 50\%$ are acceptable as cut-off for water saturation in hydrocarbon reservoirs. Above 50% implies lesser hydrocarbon volume for extraction which hence reduces the economic viability of the reservoir [19].
Volume of shale (V_{sh}) was determined using equation (10) [11] given by:

$$V_{sh} = 0.33\ [2\ (2 * I_{gr}) - 1.0] \tag{10}$$

where: V_{sh} is the volume of the shale and I_{gr} is the equation for gamma-ray index, given by:

$$Igr = (GR_{log} - GR_{min}) / (GR_{max} - GR_{min}) \tag{11}$$

According to [10], volume of shale can be classified as follows: $V_{sh} \leq 5\%$ is clean sand while $5\% < V_{sh} \leq 15\%$ is slightly shaly sand. $15\% < V_{sh} \leq 25\%$ is shaly sand while $25\% < V_{sh} \leq 35\%$ is very shaly sand. $V_{sh} > 35\%$ is shale.
Depleted oil reservoirs are commonly considered suitable candidates for carbon sequestration due to their favourable reservoir conditions and proven storage integrity. Accordingly, the effect of shale on carbon sequestration was assessed by first evaluating reservoir petrophysical properties and their suitability for hydrocarbon production and storage. These properties were then interpreted in the context of the reversible CO_2–H_2O–shale geochemical mechanisms described in Equations (1)–(5). This integrated approach provides insight into how shale content influences CO_2 storage capacity, either enhancing or limiting sequestration potential.

3. Results and Discussion

The eight (8) wells analysed displayed unique profiles of their potential reservoirs and hydrocarbon-bearing zones. These zones are defined as reservoir flags and pay flags, respectively. In all wells, regions of higher pay flags in reservoir flags were identified as potential productive reservoirs and hence suitable for carbon sequestration.

3.1. Reservoir delineation

Depth profiles of all 8 wells and corresponding reservoir delineations are presented in Table 1.

Table 1: Delineated Reservoirs and Depth Profile of Wells within the G-Oil Field

S/N	Well Code	Depth (ft)		Reservoirs delineated
		Top	Bottom	
1	IOA_13	1950.11	2748.99	4
2	IOA_14	0.00	2757.22	1
3	IOA_15	0.00	2950.48	2
4	IOA_16	0.00	2954.73	2
5	IOA_17	1084.48	2540.66	3
6	IOA_18	0.00	2799.99	2
7	IOA_19	0.00	2731.47	2
8	IOA_52	1550.06	3909.97	2

Reservoir and pay flags (see Appendix 1-8) have shown consistent alignment under all three reservoir characteristics (Porosity, Water Saturation and shale volume). Such consistency enhances accurate delineation of hydrocarbon reservoirs within the wells. Notably, this correlates with the porosity/water saturation algorithm delineation as applied in the IP software.

3.2. Petrophysical parameters

Data obtained from curve statistics of well logs were collated per reservoir (Table 2). Key production petrophysical parameters within all 18 reservoirs revealed the quality of the reservoirs being studied.

Table 2: Petrophysical parameters across wells and reservoirs within the G-Oil field

Well code	Reservoir	Total Porosity ($Ø_t$)	Effective Porosity ($Ø_{eff}$)	Water saturation (S_w) (Archie)	Water Saturation (S_w) (Indonesian)	Shale Volume (V_{sh})	Permeability (k) (mD)
IOA_13	Reservoir 1	0.238	0.21	0.467	0.457	0.256	425.446
	Reservoir 2	0.206	0.179	0.438	0.403	0.249	677.581
	Reservoir 3	0.264	0.245	0.217	0.198	0.169	2,356.49
	Reservoir 4	0.166	0.156	0.261	0.246	0.098	831.532
IOA_14	Reservoir 1	0.288	0.27	0.396	0.352	0.322	1,206.23
IOA_15	Reservoir 1	0.279	0.275	0.369	0.326	0.043	1,114.88
	Reservoir 2	0.26	0.255	0.48	0.34	0.045	190.287
IOA_16	Reservoir 1	0.288	0.274	0.239	0.2	0.08	6,497.09
	Reservoir 2	0.255	0.232	0.426	0.378	0.128	311.567
IOA_17	Reservoir 1	0.285	0.274	0.373	0.325	0.119	967.861
	Reservoir 2	0.266	0.255	0.438	0.439	0.125	181.01
	Reservoir 3	0.168	0.168	0.14	0.131	0.005	7,942.09
IOA_18	Reservoir 1	0.268	0.251	0.38	0.339	0.115	3,058.10
	Reservoir 2	0.258	0.252	0.176	0.156	0.035	4,459.96
IOA_19	Reservoir 1	0.27	0.266	0.327	0.289	0.101	848.053
	Reservoir 2	0.256	0.252	0.39	0.297	0.105	513.63
IOA_52	Reservoir 1	0.155	0.149	0.46	0.401	0.077	259.919
	Reservoir 2	0.144	0.142	0.357	0.304	0.03	215.204
Cut-off		0.4	0.4	0.5	0.5	0.5	100
Mean Values		0.240	0.228	0.352	0.310	0.117	1780.941

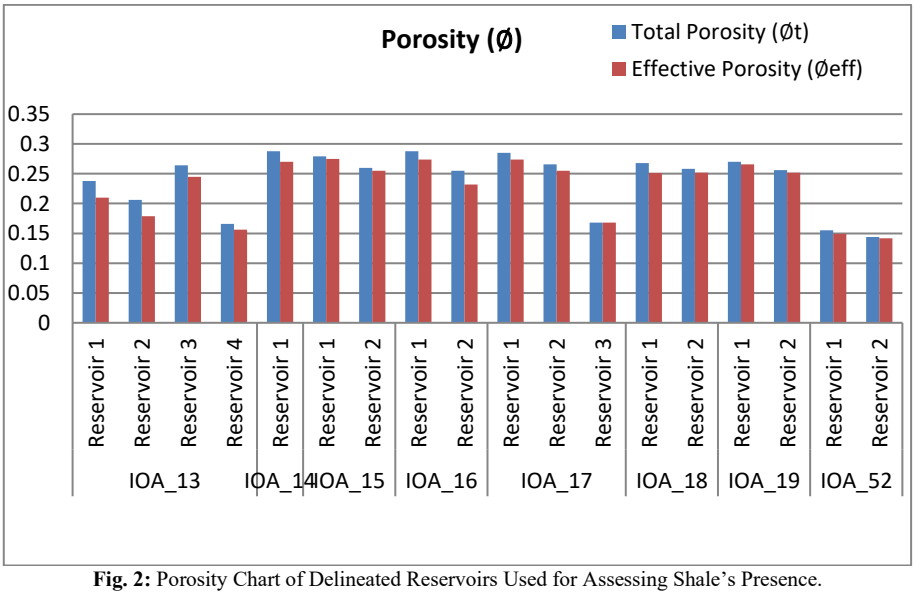

Fig. 2: Porosity Chart of Delineated Reservoirs Used for Assessing Shale's Presence.

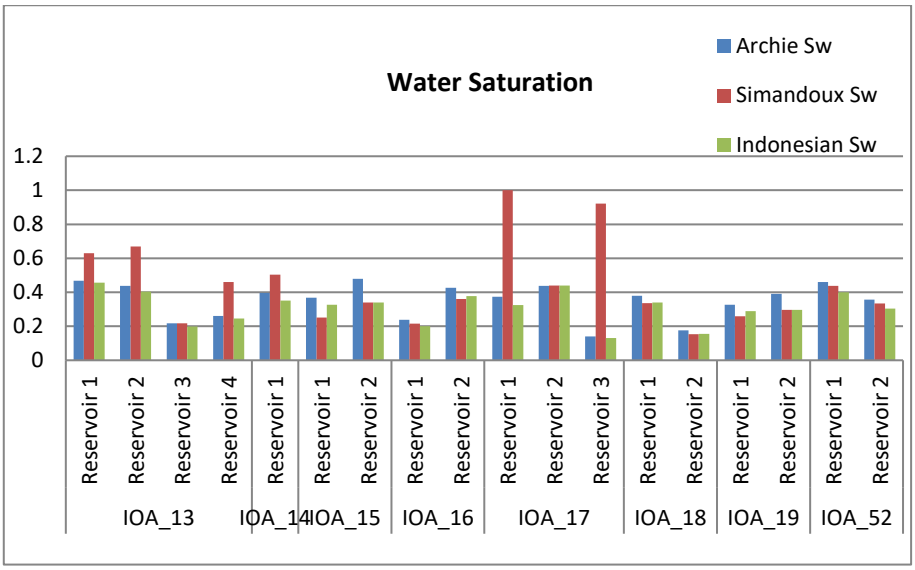

Fig. 3: Water Saturation Plot Used for Analysing Shale's Presence within Delineated Reservoirs.

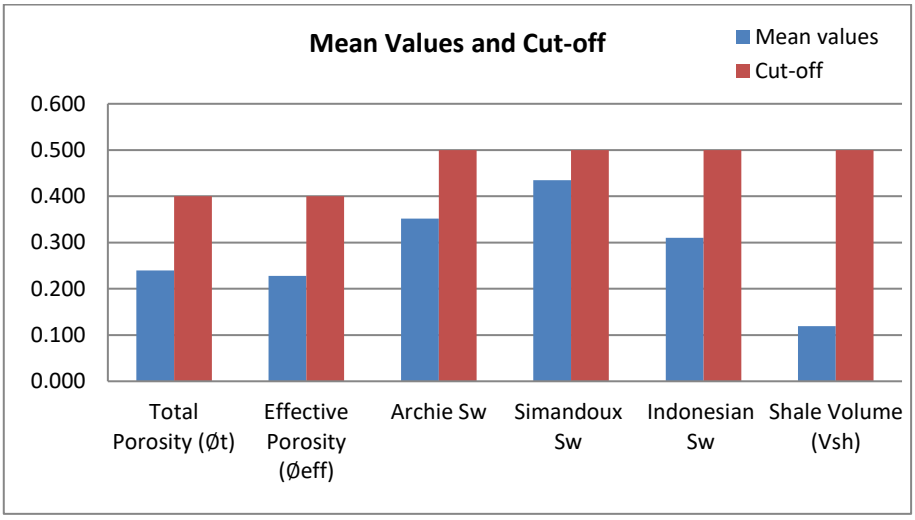

Fig. 4: Mean Values and Cut-Off of Petrophysical Parameters Reflecting Reservoirs' Quality.

The mean values of Archie water saturation (S_w), Indonesian S_w, total porosity ($Ø_t$), effective porosity ($Ø_{eff}$), permeability (k), and shale volume (V_{sh}) (Table 2; Fig. 4) fall within acceptable cut-off limits. This indicates economic viability and a strong potential for effective hydrocarbon production and CO_2 sequestration [19], provided that other reservoir conditions are favourable.

The porosity distribution of the reservoirs is illustrated in Fig. 2, showing both total porosity ($Ø_t$) and effective porosity ($Ø_{eff}$). Sixteen out of the eighteen reservoirs exhibit higher total porosity than effective porosity. The mean values of $Ø_t$ and $Ø_{eff}$ are 0.240 and 0.228, respectively (Table 2), confirming that $Ø_t$ consistently exceeds $Ø_{eff}$. Based on the classification of [17], the porosity of the study area ranges from good to very good. The higher total porosity reflects the presence of shale, which adversely affects effective porosity by introducing unconnected pore spaces. Total porosity includes shale-associated pores that are largely isolated, whereas effective porosity accounts only for interconnected pores and excludes shale-related porosity. Two reservoirs display identical values of c_t and $Ø_{eff}$, suggesting negligible shale content and indicating clean (Archie) reservoir conditions.

Figure 3 compares Archie water saturation with Indonesian water saturation. The mean Archie S_w is 0.352, while the mean Indonesian S_w is 0.310. The Archie model assumes a clean sand reservoir. This assumption neglects shale effects, leading to an overestimation of S_w due to the contribution of conductive clay minerals to bulk conductivity. Consequently, it attributes both clay and water conductivity solely to formation water. In contrast, the Indonesian model accounts for shale content by separating the conductive effects of clay minerals from true water saturation. As observed in Fig. 3, Archie S_w values are consistently higher than Indonesian S_w values, confirming the presence and influence of shale within the reservoirs. An exception occurs in well IOA_17, Reservoir 2, where both S_w estimates are approximately equal, indicating a clean, shale-free formation. Importantly, all S_w values are below the 50% cut-off, placing the reservoirs within an acceptable range for carbon sequestration.

The study area exhibits a mean permeability of 1780.941 mD, indicating excellent pore connectivity and fluid transmissibility. All eighteen reservoirs fall within the very good to excellent permeability classification according to [20]. High permeability suggests strong reservoir productivity and favourable conditions for CO_2 injection and migration.

Shale volume analysis indicates that the reservoirs range from clean sand to shaly sand. Five reservoirs are classified as clean sands, while thirteen are shaly sands, consistent with the classification of [10]. The mean V_{sh} value of 0.117 (11.7%) corresponds to a slightly shaly sand lithology. Reservoirs of this type are generally considered favourable for carbon sequestration due to their balance of porosity, permeability, and limited shale content.

Considering the low V_{sh}, moderate S_w, very good Ø, and excellent k, the oil field demonstrates favourable conditions for CO_2 sequestration. However, the interaction between shale and other petrophysical parameters and its net effect on sequestration efficiency requires further clarification.

3.3. Implications of geochemical reactions between CO_2, shale, and reservoir properties

The CO_2 solubility equations (Eqs. 1–5) describe the interaction of CO_2 with formation water and shale and explain how these reactions influence effective porosity and permeability. Shale content within the reservoirs is predominantly within the slightly shaly classification. The mean water saturation of approximately 31% provides sufficient water for CO_2 dissolution and subsequent formation of Dihydrogen Carbonate acid (H_2CO_3). This level of water saturation is adequate to sustain the reversible reactions until chemical equilibrium is reached, resulting in reservoir stabilisation.

Given the relatively low mean shale volume (11.7%), equilibrium between CO_2, water, and shale minerals is expected to be achieved over a shorter timescale. The reaction between Dihydrogen Carbonate acid and calcium carbonate ($CaCO_3$) present in shale promotes mineral dissolution, leading to the development of additional microporosity. This process involves the precipitation and redistribution of calcium and other mineral constituents, which can clog existing shale nanopores while enhancing connected pore networks. Consequently, unconnected pores are reduced, and effective porosity and permeability are increased. Unlike the conventional negative impact of shale on hydrocarbon reservoirs—where $\emptyset_{eff}$ is often reduced—these geochemical reactions during CO_2 sequestration may enhance both $\emptyset_{eff}$ and k. It should be noted, however, that the magnitude and direction of these changes are strongly dependent on the amount of available water saturation.

4. Conclusion

Petrophysical analysis confirms the presence of shale within the reservoirs, as evidenced by a higher mean total porosity (24.0%) compared to effective porosity (22.8%) and higher Archie water saturation (35.2%) relative to Indonesian water saturation (31.0%). The high mean permeability (1780.941 mD) indicates well-connected pore systems conducive to CO_2 migration and storage. A mean shale volume of 11.7% suggests a slightly shaly sand lithology. The combination of adequate water saturation and low shale content indicates favourable conditions for carbon sequestration.

Geochemical interactions between CO_2, shale, and formation water are expected to directly influence effective porosity and permeability by increasing both parameters. Adequate water saturation (31.0%) supports continuous formation of Dihydrogen Carbonate acid (H_2CO_3), which reacts with shale minerals until equilibrium is attained. The resulting increase in $\emptyset_{eff}$ and k suggests enhanced reservoir CO_2 storage potential. Based on the data obtained, shale plays a significant role in carbon sequestration due to its influence on key petrophysical parameters.

In summary, the G-oil field is considered suitable for CO_2 sequestration. It is therefore recommended that the Nigerian government and multinational companies harness the economic and environmental benefits associated with carbon sequestration in this field.

Acknowledgement/ Conflict of Interest

Thanks to Dr. Okechukwu Agbasi for guidance on the use of Interactive Petrophysics (IP) software.
There is no conflict of interest

References

[1] Chadwick A, Arts R, Bernstone C, May F, Thibeau S, et al (2008). Best practice for the CO_2 storage in saline aquifers – Observations and guidelines from the SACS and CO_2STORE projects. British Geological Survey. 267. https://www.researchgate.net/publication/284301116.

[2] Lawton D (2010). Carbon capture and storage: Opportunities and challenges for geophysics. Canadian Society of Exploration Geophysicists. 35(6). https://cseg.ca/carbon-capture-and-storage-opportunities-and-challenges-for-geophysics/.

[3] Payton RL, Fellgett M, Clark B, Chiarella D, Kingdon A, et al. (2020). UKGEOS PNM Supporting Data. Royal Holloway.

[4] Hazra B, Visharl V, Sethi C, Chandra D (2022). Impact of supercritical CO_2 on shale reservoirs and its implication for CO_2 sequestration. Energy & Fuels. 36 (17) 9882 – 9903. https://doi.org/10.1021/acs.energyfuels.2c01894.

[5] Eigbe PA, Ajayi OO, Fadipe OL, Efe S, Adelaja AO (2023). A general review of CO_2 sequestration in underground geologic formations and assessment of depleted hydrocarbon reservoirs in the Niger Delta. Applied Energy. 350. https://doi.org/10.1016/j.apenergy.2023.121723.

[6] Koehn L, Romans BW, Pollyea RM (2023). Assessing reservoir performance for geologic carbon sequestration in offshore saline reservoirs. Royal Society of Chemistry. (2) 2069–2084. https://doi.org/10.1039/D3YA00317E.

[7] Jiaping TA, Siwei MA, Dongxu LB, Zhenhua RC, He LA, et al. (2023). Analysis of CO_2 effects on porosity and permeability of shale reservoirs under different water content conditions. Geoenergy Science and Engineering. 226. https://doi.org/10.1016/j.geoen.2023.211774.

[8] Fatah A, Amao A, Abu-Mahfouz IS, Al-Yaseri A (2023). Geochemical reactions of high total organic carbon oil shale during CO_2 treatment relevant to subsurface carbon storage. Energy & Fuels. 38(2) 1161–1172. https://doi.org/10.1021/acs.energyfuels.3c03958.

[9] Goodman A, Kutchko B, Sanguinito S, Natesakhawat S, Cvetic P, et al. (2018). Reactivity of CO_2 with Utica, Marcellus, Barnett, and Eagle Ford shales and impact on permeability. Energy & Fuels. https://doi.org/10.1021/acs.energyfuels.1c01995.

[10] Adagunodu A, Bayowa O, Alatise OE and Oshonaiye AO (2021). Characterisation of reservoirs and depositional study of J-P field, shallow offshore of Niger Delta, Nigeria. Scientific African. 15. https://doi.org/10.1016/j.sciaf.2021.e01064.

[11] Emudianughe JE, Eze PM, Urah S (2021). Porosity and Permeability Trend in Agbami-Field Using Well Log, Offshore, Niger Delta. Communication in Physical Sciences. 7(4) 531 – 541. https://journalcps.com/index.php/volumes/article/view/479.

[12] Ugbor CC, Obumselu CA, Ogboke JO (2022).Evaluation of the influence of shale on the petrophysical properties of hydrocarbon-bearing reservoir sand in 'CAC' Field in the Niger Delta, Nigeria. International Journal of Geosciences. 13, 71-92. https://doi.org/10.4236/ijg.2022.131005.

[13] Ojo AC, Tse AC (2016). Geological characterisation of depleted Oil and Gas reservoirs for carbon sequestration potentials in a field in the Niger Delta, Nigeria. Journal of Applied Science and Environmental Management. 20(1), 45–55. https://doi.org/10.4314/jasem.v20i1.6.

[14] Short KC, Stauble AJ (1967). Outline of the geology of the Niger Delta. American Association of Petroleum Geologists Bulletin. 5(5), 761-779.

[15] Doust, H. and Omasola, E. (1989). Niger Delta. Edited in Edwards, J. D., and Sandtogrossi, P. A., Divergent/passive Margin Basins; American Association of Petroleum Geologists Bulletin. 48, 239-248. https://doi.org/10.1306/M48508C4.

[16] Umar BA, Gholami R, Nayak P, Shah AA, Adamu H (2020). Regional and field assessments of potentials for geological storage of CO_2: A case study of the Niger Delta Basin, Nigeria. Journal of Natural Gas Science and Engineering. 77. https://doi.org/10.1016/j.jngse.2020.103195.

[17] Agada, I. O., Igboekwe, M. U., Amos-Uhegbu, C. and Aigba, P. I. (2025). Petrophysical Analysis of Reservoir Quality using Key Production Parameters: A Case Study of the G-Oil Field within the Niger Delta Basin. Nigerian Journal of Theoretical and Environmental Physics. 3(3), 68-80. https://doi.org/10.62292/njtep.v3i3.2025.98.

[18] Tixier MP (1949). Evaluation of permeability from electric log resistivity gradients. Oil and Gas Journal. 8, 75-90. https://www.semanticscholar.org/paper/Evaluation-of-permeability-from-electric-log-Pierre/6326da9fdf97b066c4d8ab553bba082175576438.

[19] Fozao KF, Djieto-Lordon AE, Ali EAA, Agying CM, Ndeh DM, et al. (2019). Analysis of shaly sand reservoir rocks in the eastern Niger Delta Basin using geophysical well logs. Journal of Petroleum and Gas Engineering. Vol. 10(1), 1-13. https://doi.org/10.5897/JPGE2018.0300.
[20] Bachu B (2007). `Screening and ranking of hydrocarbon reservoir for CO_2 storage in Alberta Canada. https://www.researchgate.net/publication/237408831Accessed July 2025.

Appendix

Appendix 1

Reservoir Pay Model of Well IOA_13 showing 4 delineated reservoirs

Appendix 2

Reservoir Pay Model of Well IOA_14 showing 1 delineated reservoir

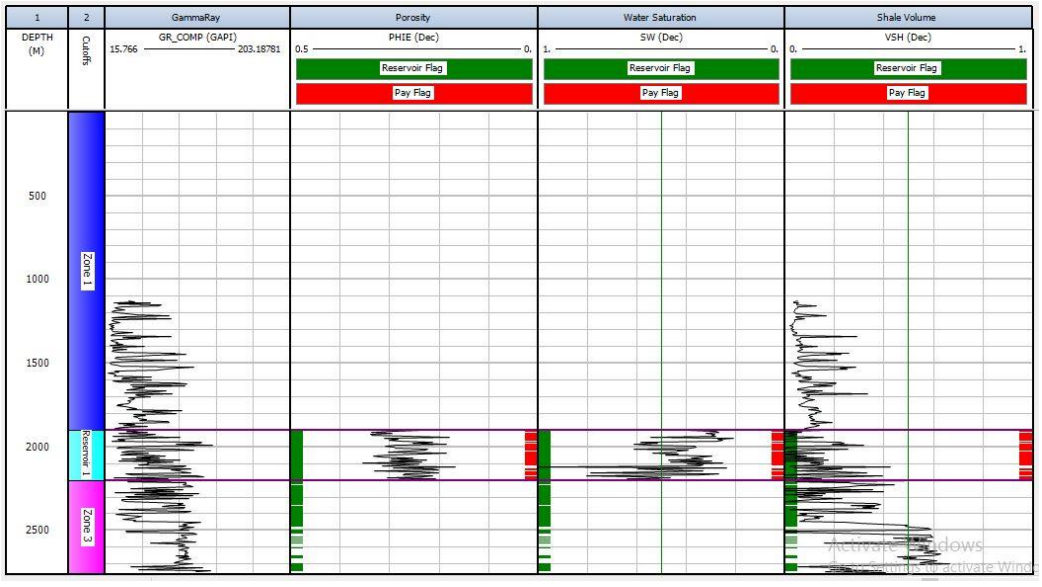

Appendix 3

Reservoir Pay Model of Well IOA_15 showing 2 delineated reservoirs

Appendix 4

Reservoir Pay Model of Well IOA_16 showing 2 delineated reservoirs

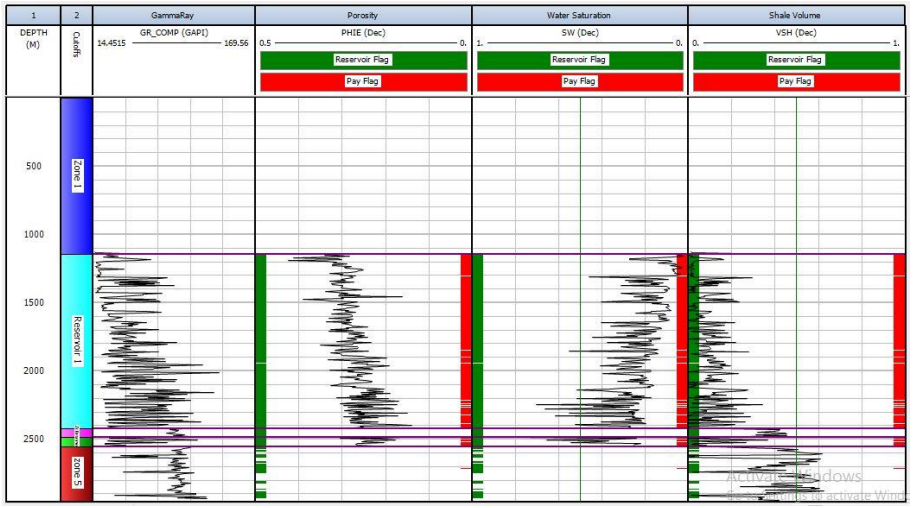

Appendix 5

Reservoir Pay Model of Well IOA_17 showing 3 delineated reservoirs

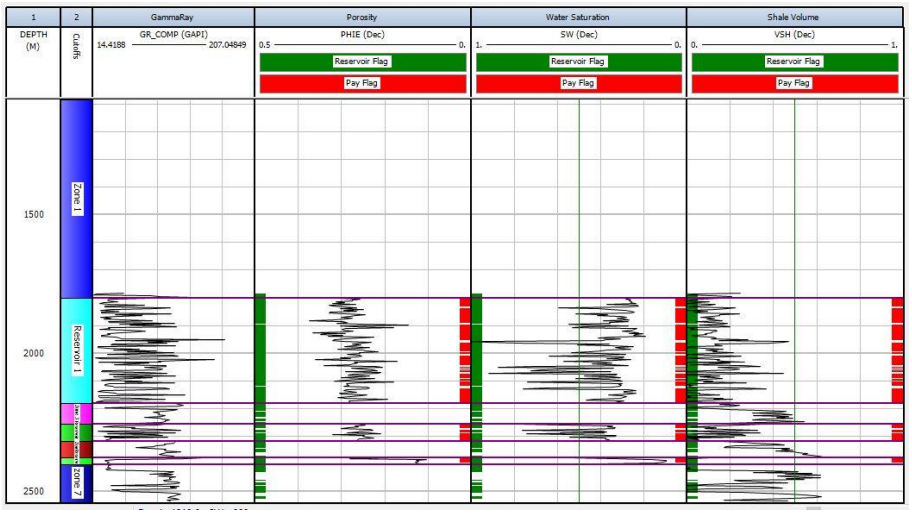

Appendix 6

Reservoir Pay Model of Well IOA_18 showing 2 delineated reservoirs

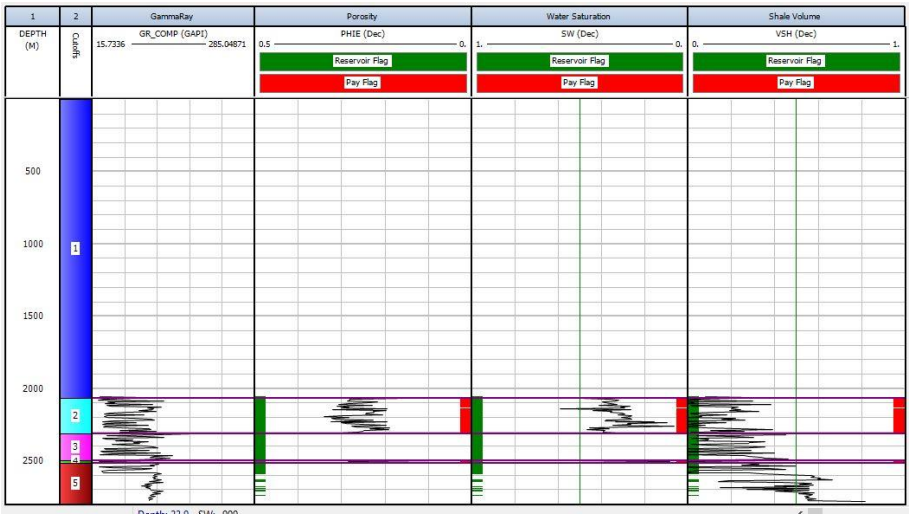

Appendix 7

Reservoir Pay Model of Well IOA_19 showing 2 delineated reservoirs

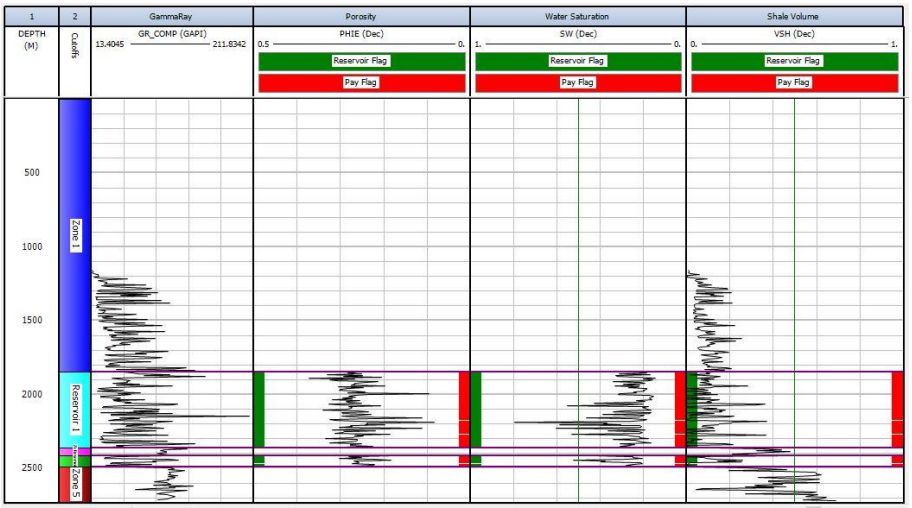

Appendix 8

Reservoir Pay Model of Well IOA_52 showing 2 delineated reservoirs